Retrofitting of Damage Rail Bridge Girder and Its Performance Evaluation

Anjani Kumar Shukla, P. R. Maiti & Gopal Rai

Journal of Failure Analysis and Prevention

ISSN 1547-7029
Volume 20
Number 3

J Fail. Anal. and Preven. (2020)
20:895-911
DOI 10.1007/s11668-020-00890-1

Springer

J Fail. Anal. and Preven. (2020) 20:895–911
https://doi.org/10.1007/s11668-020-00890-1

TECHNICAL ARTICLE—PEER-REVIEWED

Retrofitting of Damage Rail Bridge Girder and Its Performance Evaluation

Anjani Kumar Shukla · P. R. Maiti · Gopal Rai

Submitted: 7 April 2020 / Published online: 12 June 2020

Abstract Strengthening of prestressed girder using FRP has rarely been performed because prestressed girder has excellent strength under service load in both tension and compression. In this study, retrofitting of a 59-year-old prestressed bridge of Indian railway at Ratlam has been executed in which multiple vertical cracks visualized in tension zone and surface deterioration were observed. Due to this, deterioration speed of the trains over the bridge was restricted up to 20 km/h. The PSC girders of the bridge were strengthened by using prestressed carbon fiber. Serviceability of the structure was monitored before strengthening and after strengthening of the bridge girder. Deflections and natural frequencies after strengthening of girder were monitored for 481 days to ascertain the improvement and consistency in behavior of girder. After strengthening, the considerable decrement in deflection was noted by dint of the speed limit of the train which is recommended to increase up to 100 km/h.

Keywords Damaged girder · PSC girder · CSi bridge analysis · Strengthening · Retrofitting · Prestressed carbon fiber

A. K. Shukla (✉) · P. R. Maiti · G. Rai
Department of Civil Engineering, Indian Institute of Technology (BHU), Varanasi, India
e-mail: akshukla.rs.civ16@iitbhu.ac.in

A. K. Shukla · P. R. Maiti · G. Rai
Dhirendra Group of Companies, Mumbai, India

Introduction

The strengthening of concrete structure with carbon fiber-reinforced polymer (GFRP) is a well-established retrofitting method, and also glass fiber-reinforced polymer (GFRP) can contribute to the strength of tension zone of concrete structure by increasing the flexure strength. If the steel ratio is comparatively smaller in reinforced concrete structure, then the flexural strength of concrete attains a good value when fixed with GFRP plate and also the crack size in the old structures can be reduced by application of plates in all types of loading conditions. A very important characteristic which degrades the quality of the strengthened structure is reduction in ductility caused by gluing of plate, because it is certain that plates reduced the elasticity of structure. And it brings the reason of failure of concrete layer between longitudinal reinforcement and GFRP plate at limiting load [1]. The least strong element in the sandwich of concrete and fiber plate determines the shear strength of CFRP and adhesive interface. In this study, it is proved that the CFRP contribution is much more effective in stiffness of beam rather than the strength [2]. Vertical deflection and steel reinforcement stress were significantly reduced by the use of GFRP, and the moment of inertia also improved in the concrete structures by using glass sheet [3]. New fiber composite material for reinforcing concrete (NEFMAC) grid, a type of FRP invented in Tokyo, can be a replacement for steel reinforcement, but several parameters like modulus of elasticity, brittleness of FRP and cross section area of NEFMAC FRP have higher values than steel which will need to be anchored [4]. With the help of CFRP plate, the stiffness in corroded and damaged steel girder can be restored up to 10–37%, and to prevent the galvanic corrosion a glass fabric layer can be

used. After strengthening of girder with carbon and glass fiber, the global flexural of girder was improved by 11.6% compared to strengthened girder [5]. This strength can be verified by the case study of Horsetail Creek Bridge. After FRP strengthening of Horsetail Creek Bridge, the capacities on mass proportion and scaled truck loading improved by 28 and 37%, respectively. Yield of steel bars and crack length are reduced in FRP-strengthened bridge, and the mode of failure of bridge changed from shear failure to flexure failure [6]. The restrainer made by FRP of glass carbon and combining glass and fiber has reduced the impact at hinge, so it may be used as a device for earthquake restrainer in bridges. When these carbon and fiber FRP restrainers were compared with steel, they showed least movement than steel restrainer [7]. The impact factor of FRP bridge based on deflection is much lesser than of concrete bridge which explains that dynamic impact factor suggested in AASHTO [8] can also be applied to FRP bridge and in its strength design, while the acceleration of fiber-reinforced bridge is higher comparatively to concrete bridge [9]. Modeling of a beam strengthening with FRP using 3D finite element simulation, compared to experimental analysis of beam in both linear and nonlinear, showed that final failure load from finite element analysis is lesser than the experimental load by 6–18% [10]. By the full-scale load test of strengthened T-type bridge girder using concrete weight block as loading system, it is found that this method is safe and convenient and for strengthening with this method the FRP materials carbon, glass and aramid fiber were found effective in improving flexure capacity. The design code ACI 440.1R, which is a USD concrete, is used for strengthening, and it concludes that ACI 440.1R can be used for full-scale bridge strengthening [11]. The beam and slabs which contain prestressed CFRP tendons show much lower deflection and better serviceability control than the steel-reinforced structures [12]. For the anchoring of plates, there are three different anchorage systems available: (a) discontinuous mechanical anchorage system (DMA), (b) sandwich discontinuous mechanical anchorage system (SDMA) and (c) additional horizontal strip (HS). The studied result explains that SDMA system is more successful than DMA and HS systems, respectively. The sandwich discontinuous mechanical anchorage system improves the shear strength by 59–91% altering the failure by deboning of FRP [13]. The externally bonded FRP performed well under transient loading. CFRP and concrete showed the properties of a good composite material together. It is also noticed that transient loading affects the final ultimate performance if loaded during curing period [14]. Flexural strengthening by CFRP strip gave 16, 19 and 24% additional strength than unstrengthened structure in case of cracking, yielding and on ultimate load capacity, respectively, and failure of structure occurs as tensile failure which means bonding of epoxy with concrete and CFRP was adequate [15].

In this study, inspection and analysis of damaged railway of four-span bridge were carried out followed by the design of retrofitting material. It is found that span 2 and span 4 were highly damaged while in span 1 and 3 no such damaged reported. The strength analysis of bridge girder before retrofitting was performed, and prestressed CFRP sheet was designed accordingly. After strengthening of the girder, the deflection and natural frequency were calculated under static and moving locomotive over the bridge. The results of span no. 1 have been assumed for full-scale capacity of the bridge. The study concludes that deflection decreases and natural frequency increases; as a result, speed limit increases from 20 to 100 kmph. To calculate the total deflection of bridge girder, the contribution of the deflection of girder due to bending and deflection of girder due to shear has to be considered. Total maximum deflection at mid-span due to WAGON 7 locomotive can be written as follows:

$$\delta = \delta_{\text{bend}} + \delta_{\text{shear}}$$

where δ = total deflection of bridge girder.

Background

Bridge no. 114 was constructed on Khan River during 1958–1960. The bridges have composite PSC I girders supported on neoprene bearing (Fig. 1). The main reason for retrofitting of the PSC I girders on the bridges is the development of cracks on the girders. As the cracks were propagating with time, immediate strengthening of these girders is required to arrest further deterioration.

All the details and drawings are based on the observations from the site visit, and after calculating the design strength of the bridge, strengthening of PSC I girders is proposed. A site visit carried out is indicated at the severity of cracks on the PSC I girders. Also, separation of diaphragm from girders and spalling of concrete at deck slab were observed at several locations (Fig. 2).

Based on the strengthening design for the PSC I girders, it is proposed with the help of prestressed carbon laminates and carbon fiber wrapping. The complete analysis results, design, drawings and methodology of strengthening are presented in this study. Line diagram of bridge section is shown in Fig. 3, and the details of the bridge are listed in Table 1.

Damage Detection of Bridge Girder

1. The PSC I girders show vertical cracks from the bottom of the girder in span S2, S3 and S4.

Fig. 1 Site view of raw bridge no. 114

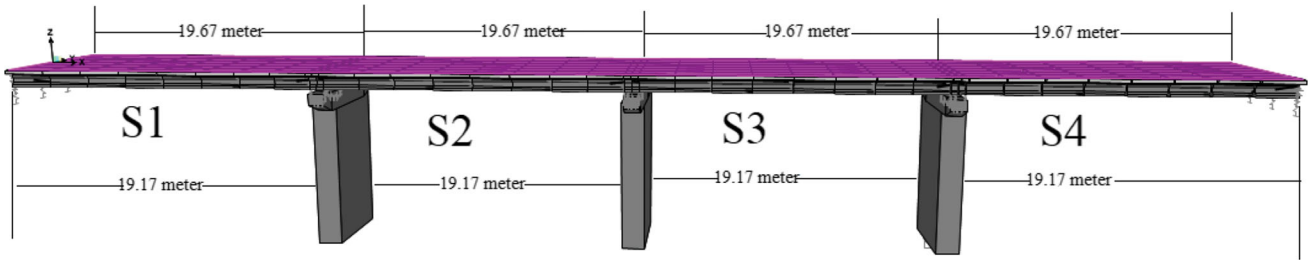

Fig. 2 Schematic of the bridge no. 114

Table 1 Details of bridge no. 114 (upstream)

S. No.		Details
1	Clear span	18.15 m
2	Effective span	19.17
3	Overall length of girder	19.67 m
4	Overall length of deck slab	20.10 m
5	Diaphragm details	6 (4 intermediate and 2 end)
6	Total weight of girder (per span)	145 T (girders + deck slab + diaphragms)
7	Details of track	Rail—60 kg, Sleeper—PSC
8	Bank height in approaches	9.25 m
9	Thickness and width of the deck slab	Thickness—200 mm, width—4300 mm
10	Substructure type and material type	Stone masonry in cement mortar, gravity-type substructure

2. Discoloration due to deterioration with time is seen in the overall structure (Fig. 4).
3. Severe deterioration of the diaphragm observed.
4. Severe spalling and corroded reinforcement exposure is observed at the bottom slab. This may be attributed to the carbonation taken place in the structure (Fig. 5).
5. Spalling of concrete is observed in diaphragm bottom.
6. Cracks at the girder bottom at bearing locations are observed.
7. Severe deterioration at intermediate span locations is seen.
8. Termite attack is observed in the girders.

Load Test Vehicle

The WAGON-7 rail engine of Indian railways was made to run over the bridge to record the deflections and

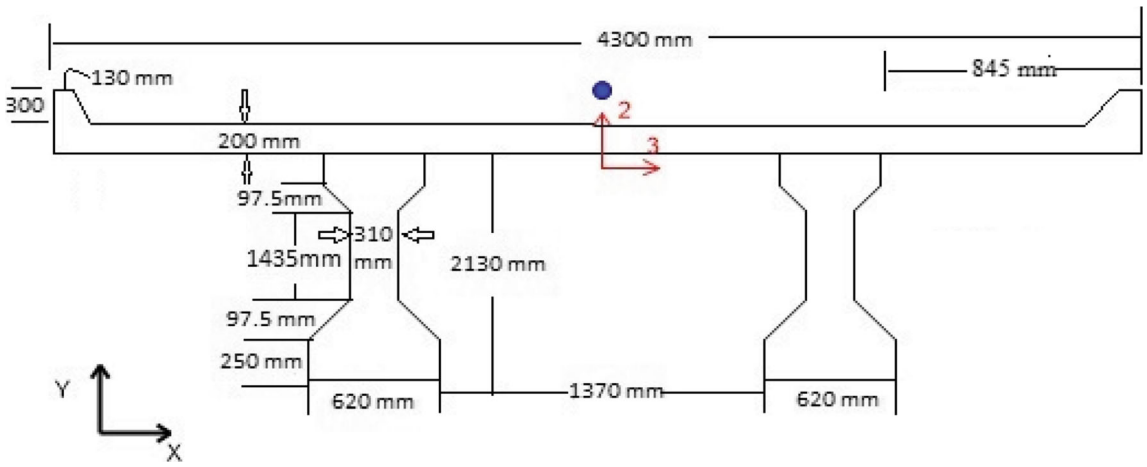

Fig. 3 Line diagram of girder

Fig. 4 Surface de-coloration and deterioration

Fig. 5 Cracks and delamination at locations of bearings

Table 2 Major parameters of loading vehicle

S. No.	Parameter	Units	Values
1	Weight of vehicles	Tons	123
2	Total no. of axles	Tons	6
3	Axle load	Tons	20.5
4	Max design speed	km/h	110
5	Buffing load	Tons	400
6	Lateral force/axle	Tons	4
7	Dynamic augment	%	≤ 50
8	Unsprung mass/axle	Tons	4.3

All the value has been taken from Indian railway (Research Designs and Standards Organisation) [16]

frequencies in the static and dynamic loading conditions at different speeds (Fig. 6). The details of WAGON 7 are listed in Table 2.

Testing of Bridge Girder Testing to detect deflection in pre- and post-strengthening state of girder was carried out using linear potentiometer (Fig. 7), and to assess the natural frequency of the beam before and after strengthening of girder, the accelerometer was used. An independent support system using steel cribs was created to place sensor.

Analytical Analysis

Three-dimensional model of the Ratlam–Godhra bridge no. 114 was modeled and is shown in Fig. 2, and the loading model of bridge by locomotive wagon 7 is represented in Fig. 8. The designing and analysis of the bridge are done with the help of CSiBridge student software and IRC:112-2011 [17] along with Indian railway track design manual.

Fig. 6 Load applied on the bridge using Wagon 7 and sensors at site

Fig. 7 Arrangement of deflection sensor and accelerometer

For example, (1) the lane is designed as a single lane with a width of 4.3 m. All the data which are given are obtained from total station survey of bridge and design manuals of Indian railways. The techniques of the bearing, bent cap, restrainer and deck slab are obtained from IRC 2011. (2) The loading of axle is redefined as per the norms of Indian rail locomotive wagon 7. Table 3 consists of the details of axle used in the designing of bridge. (3) The designed speed of locomotive was kept maximum 100 kmph followed by minimum 20 kmph, respectively, at the interval of 20 s on the track.

Table 3 Axle details of Indian rail locomotive Wagon 7

Load length type	Minimum distance (m)	Axle load (kN)	Axle width (m)
Leading load	Infinite	201.023	1.6
Fixed length	1.9	201.023	1.6
Fixed length	1.9	201.023	1.6
Fixed length	7.4	201.023	1.6
Fixed length	1.9	201.023	1.6
Fixed length	1.9	201.023	1.6
Trailing load	Infinite	201.023	1.6

Data Collection and Analysis

The data collection and analysis started with unstressed state of bridge girder with time history load case. A linear analysis with direct integration and transient time history motion has been performed. The load is applied as RAMPTH function during the designing of the load. The output time step was selected as 320 with a size of 0.05. The stress diagram obtained after applying the load is

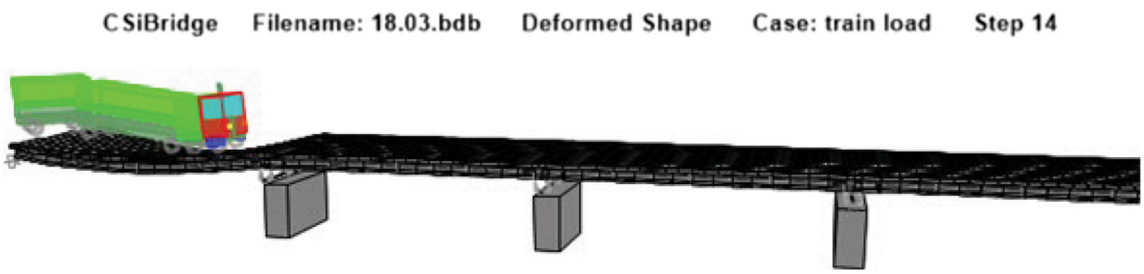

Fig. 8 Loading model of Wagon 7 locomotive

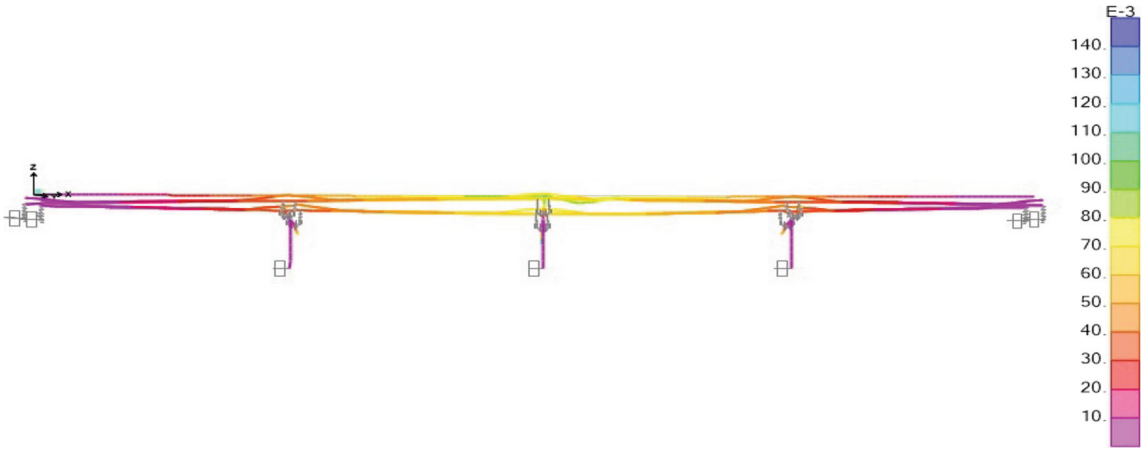

Fig. 9 Stress diagram of bridge under dynamic loading

shown in Fig. 9, which shows that maximum stress in the deck slab occurs at just before the piers and minimum at the abutments.

Measurement of Deflection and Bending Moment

The maximum deflection in the PSC I girder occurs at the mid-span. And maximum moment occurs on the girder when all the six axles were on the one girder, i.e. when locomotive completely occupied a girder. At this state, the maximum bending moments occurs (Figs. 10 and 11).

Natural Frequency For analysing the natural frequency, a new load case type 'Modal' was added to the girder with all other settings accordingly to analyze the natural frequency of the girder when the locomotive is moving in full speed of 100 kmph. The output of natural frequency is given in Table 4.

Analysis of PSC Girder Beam for Bridge

Assumptions Assume that PSC girder beams behave like a simply reinforced girder beam with no prestress left. The analysis is performed on the girder as of a simple reinforced concrete beam as the details of pre-strength forces are not available.

Strength Calculations All the necessary data for the calculation of strength of the existing girder is given in Table 5.

Retrofitting Design of Girder The existing shear and bending capacity of the girder are necessary to calculate and design the size of laminates. Table 6 contains all such details.

Capacity Evolution of Existing Structure

Shear Capacity

Percentage of reinforcement, $p = 100\ A_s/bd$

Shear strength of concrete $\tau_c = 0.71$ N/mm^2 (Table 19, IS 456:2000)

Shear contribution of concrete $V_{uc} = \tau_c bd = 1002.38$ kN. (Eq 1)

Shear contribution of shear reinforcement $V_{us} = 601.52$ kN. (Eq 2)

Adding Eqs 1 and 2, the total shear strength of the section $V_{u,all} = V_{uc} + V_{us} = 1603.90$ kN.

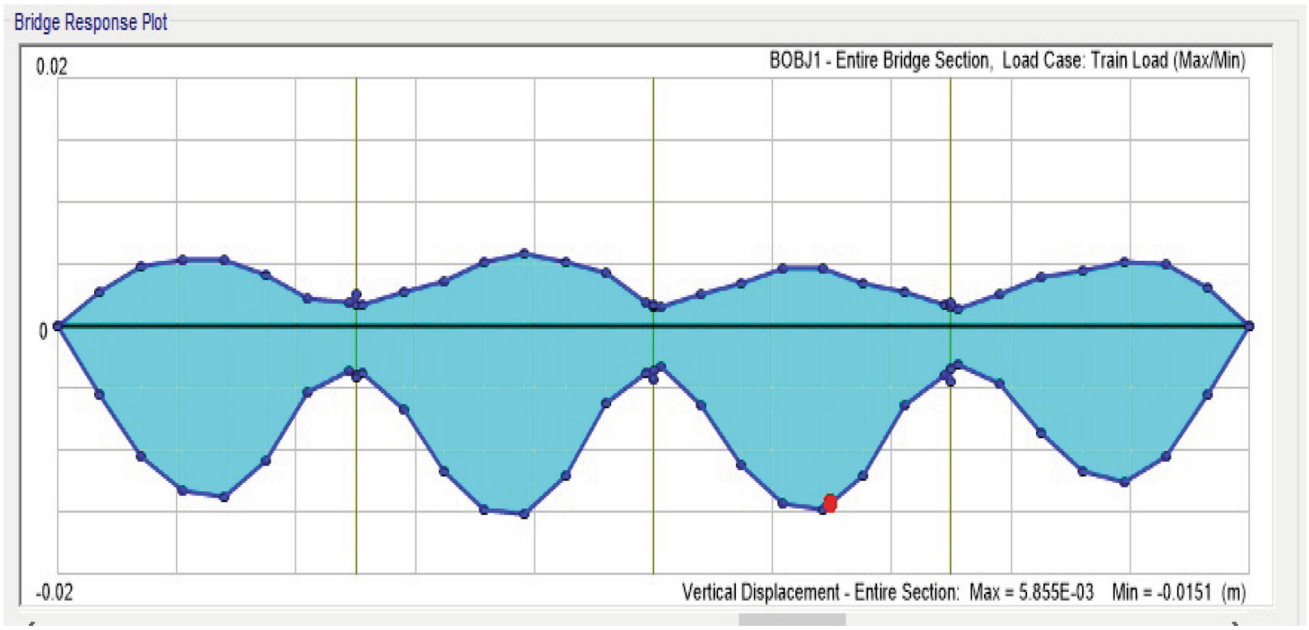

Fig. 10 Vertical displacement graph of bridge under dynamic wagon loading

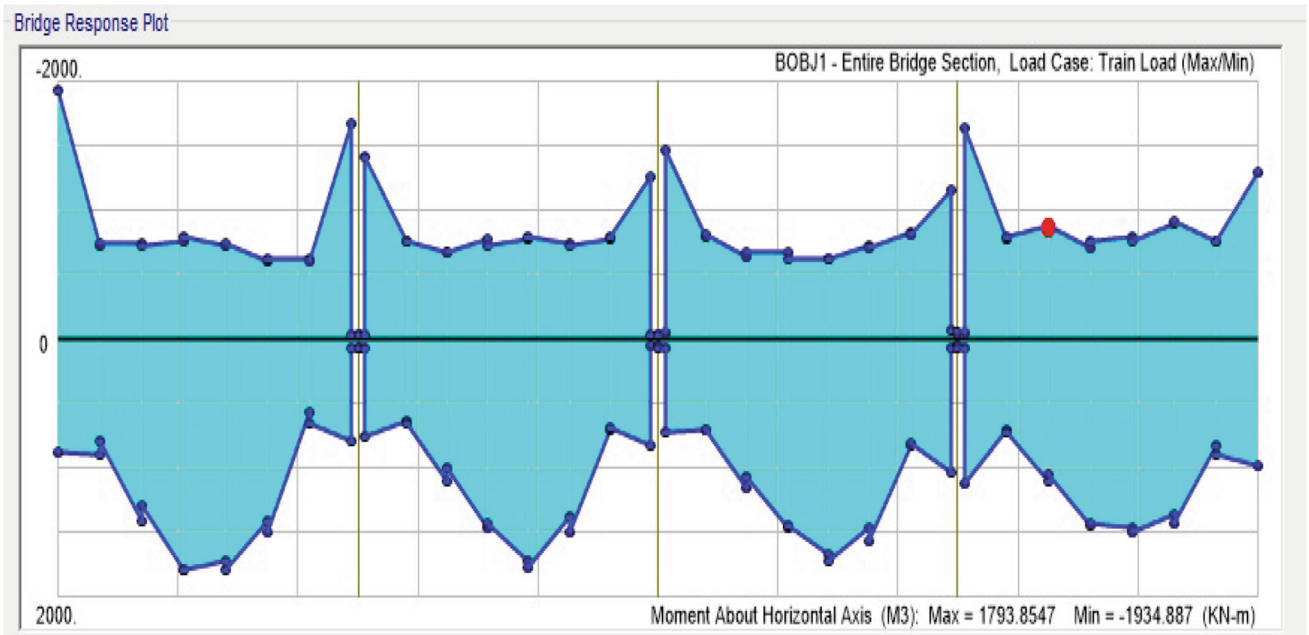

Fig. 11 Bending moment graph of bridge under dynamic wagon loading

1603.90 kN > 2085.07019 (required). Hence, the section is unsafe and the strengthening is required.

Bending Moment Capacity at Mid-Span

Neutral axis depth (from trial and error) X_u = 456.55 mm.

Strain at the level of compressive reinforcement $\varepsilon_{sc} = 0.0035 \times (X_u - d')/X_u$.

Corresponding stress in the compression reinforcement f_{sc} = 217.50 N/mm^2.

Compressive force in concrete C_c
$= 0.36 f_{ck} b X_u$, thus, $C_c = 3566.57$ kN (Eq 3)

Compressive force in compression steel $C_s = f_{sc} A_{sc}$ so C_s = 0.00 kN. (Eq 4)

Adding Eqs 3 and 4, the total compressive force $C_c + C_s$ = 3566.57 kN.

Tensile force in tension steel $T_s = 0.87 f_y A_{st}$, thus, T_s = 3566.57 kN.

Since total compressive force ($C_c + C_s$) $\approx$ total tensile force (T_s), the neutral axis depth is correct.

Moment of resistance of the section $Mu_{all}^{-} = C_c(d-0.42X_u) + C_s(d-d')$, thus Mu_{all}^{-}=7483.55 kNm < 9728 kNm (required).

Hence, the section is unsafe so strengthening is required.

Table 4 Natural frequency of bridge girder

Natural frequency				
Step (Num)	Period (s)	Frequency (cycle/s)	Circ freq (rad/s)	Eigenvalue (rad^2/s^2)
1	0.291213	3.43391768	21.57594	465.5212346
2	0.175419	5.70063227	35.81813	1282.938359
3	0.173143	5.77555921	36.28891	1316.8849
4	0.170389	5.86891367	36.87547	1359.800448
5	0.151647	6.59427051	41.43302	1716.695442
6	0.134778	7.4195864	46.61864	2173.297243
7	0.105045	9.51976239	59.81443	3577.76618
8	0.08946	11.1781368	70.23431	4932.857619
9	0.085592	11.6832967	73.40832	5388.7812
10	0.079999	12.500172	78.5409	6168.672538
11	0.079232	12.6211516	79.30103	6288.654018
12	0.061716	16.2032881	101.8083	10,364.92218

Design of Strengthening at Mid-Span

The design moment M_u^{+} = 9728 kN.

Design stress for laminates (with anchors) f_f = 1500 N/mm^2.

Let the area of the laminates required be A_f.

The neutral axis depth for the strengthened section is given by (assuming that the compression reinforcement is yielded),

$$X_{u,str} = \left(0.87 f_y A_{st} - f_{sc} A_{sc} + f_f A_f\right)/(0.36 f_{ck} b).$$

The moment carrying capacity for the strengthened section is given by

$$M_{u,str} = 0.87 f_y A_{st}\left(d - 0.42 X_{u,str}\right) + 0.87 f_y A_{sc} \times \left(0.42 X_{u,str} - d'\right) + f_f A_f \left(D - 0.42 X_{u,str}\right).$$

Now, for $M_{u,str} = M_u^{+} = 9741.92$ kNm (capacity after strengthening)

$X_u = 610.16$.

By simplifying and solving for A_f, we get the area of the laminates required as A_f = 800 mm^2.

So three prestressed laminates of size 100/2.4 and two non-prestressed laminates of size 100/2.4 at sides have been provided. The line diagram of girder lamination is shown in Fig. 12.

Shear Strengthening

The shear contribution of FRP shear reinforcement is given by

$$V_f = A_{fv} f_{fe} (\text{Sin}\ \alpha + \text{Cos}\ \alpha) d_f / s_f$$
(Clause 10.4, Eq 10.3 of ACI 440.R)

where

Table 5 Design data of girder

S. No.	Details	Value
1	The maximum positive bending moment on girder (Mud)	7460 kNm
2	Maximum shear force on girder	1671 kN
3	Critical design moment Mu1	8947 kNm
4	Limiting moment of resistance, Mu_{lim}	7459 kNm
5	Area of steel required A_{st}	16398 mm^2
6	Shear force at the critical section	1223 kN
7	Nominal shear stress	0.86 MPa
8	Shear force carried by concrete, V_c	1002 kN
9	Stirrups provided	2L—10-mm-diameter stirrups at 130 mm c/c spacing

$$A_{fv} = 2n\,t_f W_f,$$
$$f_{fe} = \varepsilon_{fe} E_f,$$
$$\varepsilon_{fe} = K_v \varepsilon_{fu} \le 0.004,$$
$$K_v = k_1 k_2 \mathrm{Le}/(11{,}900\ \varepsilon_{fu}) \le 0.75$$
$$L_e = 23{,}300/(nt_f E_f)^{0.58},$$
$$k_1 = (f_c'/27)^{2/3},$$
$$k_2 = (d_f - 2L_e)/d_f.$$

In this case, two sides wrap on full side face, so the depth of beam d_f = 2130.00 mm, thickness of ply t_f = 1 mm, E_f = 220 GPa.

Assuming the number of plies, n = 1.

f_c' = 28.00 N/mm^2 (0.8 f_{ck}), ε_{fu} = 0.0155, α = 90°. Thus, L_e = 18.567 mm, k_1 = 1.0245, k_2 = 0.9913.

Table 6 Details of laminate and girder

(a) Design load	Max. ultimate positive bending moment Mu$^-$ = 9728 kNm (considering 30% additional moment)
	Max. ultimate negative bending moment Mu$^+$ = 0 kNm
	Max. ultimate shear force V_u = 2085 kN (considering 30% additional shear)
(b) Laminate properties	Strength of FRP laminate (with anchors) f_f = 3200 N/mm^2
(c)	Section properties
	diameter = 10 mm, spacing = 130 mm
Shear reinforcement:	At mid-span:
Legs = 2,	Total depth of beam D = 2330 mm
	Effective depth of beam d = 2290 mm (assuming a clear cover of 40 mm)
	Breadth of beam b = 620 mm
	Effective cover for compression reinforcement d' = 0 mm
	Area of steel in tension A_{st} = 16398 mm^2. Area of steel in compression A_{sc} = 0 mm^2

Hence, K_v = 0.1022 ≤ 0.75 (Okay). Thus, ε_{fe} = 0.0016 ≤ 0.004 (Okay) which gives f_{fe} = 348.62 N/mm^2 < 1250 N/mm^2.

For continuous side face wrap, $w_f = s_f$. Hence, $V_f = A_{fv} f_{fe} (\mathrm{Sin}\ \alpha + \mathrm{Cos}\ \alpha) d_f / s_f$ [18].

Thus, V_f = 1486.3 kN.

Over this nominal strength, a strength reduction factor, $\Phi = 0.85$, as recommended by ACI 318 and an additional strength reduction factor, Ψ_f = 0.85, as recommended by ACI 440.2R should be applied to get the allowable shear strength due to fiber wrap.

Therefore, allowable shear strength due to wrap is $V_{uf} = \Phi \Psi_f V_f$ = 1073.85 kN > 200 kN.

Therefore, the shear strength of the section after wrapping is $V_{uc} + V_{us} + V_{uf}$ = 2677.75 (capacity after strengthening) > 2085.07 (required).

So one layer of 600 GSM Glass fiber for shear enhancement with anchor fasteners for anchorage has been provided. Figures 12 and 13 contain the proposed plan for lamination of girder.

Pre- and Post-strengthening Results

The data collection and analysis are done with the help of DGC cDAQ 9178 software for deflection. The electric signals through the cable go to the NI 9205 module which is attached to NI compact DAQ 9178 chassis, and this hardware is integrated to the cDAQ 9178 software. The data collection and analysis are done with the help of LabVIEW 2011 software of National Instruments. The signals through the cable go to the NI 9234 module, which is attached to NI cDAQ 9178 chassis, and this hardware is integrated into the LabVIEW 2011 software. As the stiffness of the girder changes, the natural frequency will also change. Accelerometers are mounted onto the girders for recording the frequency. The motion (or dynamic force) of the vibrating body is converted into an electrical signal by the vibration transducer or pickup.

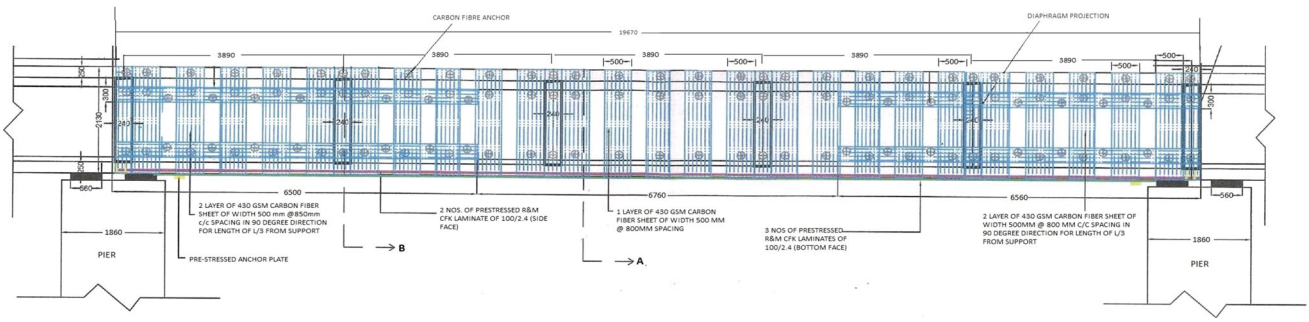

Fig. 12 Laminated model of full bridge

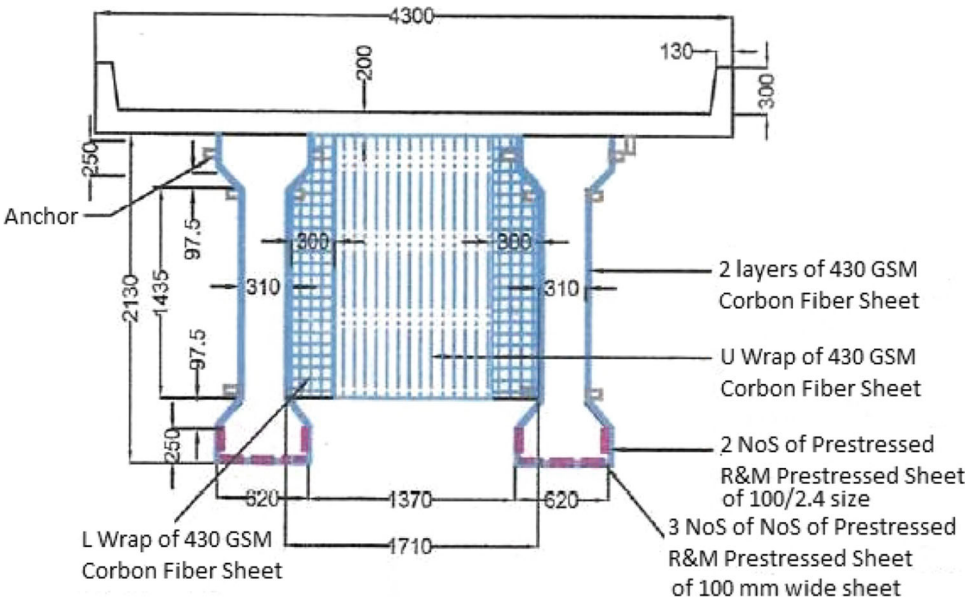

Fig. 13 Lamination of required CFRP sheet over girder as per calculation

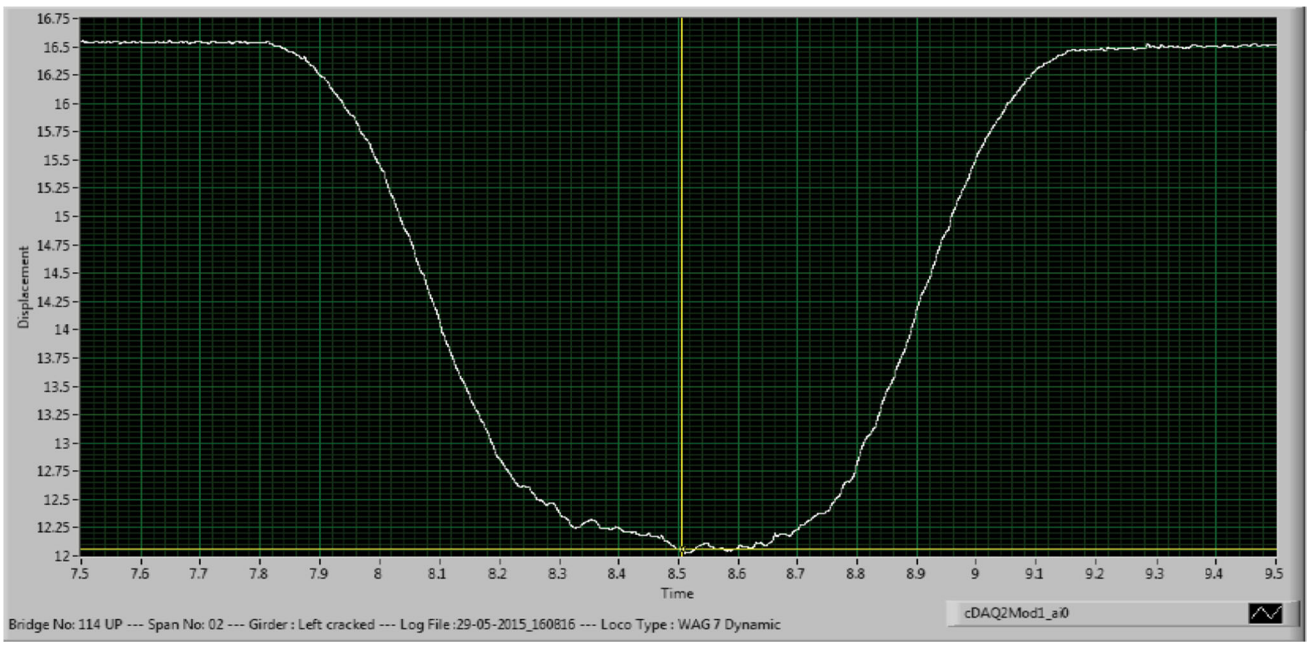

Fig. 14 Maximum deflection of cracked left girder due to dynamic load on span no. 2

The accelerometer is attached to the metal base plate using the magnetic property. Figure 14 shows the accelerometer B&K model no. 4396 used for recording the vibration. The technical specifications are given below.

Loading Condition In this study, two types of loading were considered that can be exerted by locomotive WAGON 7 of Indian railway:

(a) *Static Loading* In this case, the center of locomotive coincides with the center point of bridge girder at the time of recording the deflections and natural frequency data.

(b) *Dynamic Loading* In this case, locomotive WAGON 7 was running with a constant speed of 20 and 100 km/h over the girder for recording the deflection and natural frequency at mid-span.

A large number of results were recorded in terms of deflection and natural frequency of girder in pre- and post-strengthening states for static and dynamic loading condition. Recorded data of maximum deflection and maximum natural frequency under both static and dynamic loading conditions are presented in graphics separately for pre- and post-strengthening stages.

Table 7 Pre-strengthening test results of deflection and natural frequency

S.N.	Condition of girder	Span no.	Girder location	Type of loading	Deflection (mm)	Natural frequency (Hz)
1	Un-cracked	1	RSG	Static	2.708	…
2	Un-cracked	1	LSG	Static	2.7485	…
			Average		2.72825	
3	Un-cracked	1	RSG	Dynamic@20 kmph	2.7217	9.57
4	Un-cracked	1	LSG	Dynamic@20 kmph	2.567	9.349
			Average		2.64435	9.4595
5	Cracked	2	RSG	Static	3.3703	…
6	Cracked	2	LSG	Static	4.561	…
			Average		3.96565	
7	Cracked	2	RSG	Dynamic@20 kmph	3.304	9.066
8	Cracked	2	LSG	Dynamic@20 kmph	4.507	8.221
			Average		3.9055	8.6435
9	Cracked	4	RSG	Static	3.864	…
10	Cracked	4	LSG	Static	4.442	…
			Average		4.153	
11	Cracked	4	RSG	Dynamic@20 kmph	3.809	7.899
12	Cracked	4	LSG	Dynamic@20 kmph	4.413	8.978
			Average		4.111	8.4385

Figure 12 shows the lamination pattern of the span 2 and 4 of the bridge after retrofitting. Pre- and post-analysis of deflection and natural frequency of span nos. 2 and 4 of the bridge 114 have been recorded, and the results are produced in Tables 7 and 8. Every span has two girders named left-side girder (LSG) and right-side girder (RSG) for all data-recording purposes.

(i) Pre-strengthening test results

Before strengthening, the deflection and natural frequencies were collected by applying the load on every span separately. Some of the graphical figures among them with the highest value on respective girder were represented in the figure.

An independent platform of steel cribs was provided at the site for the placement of the linear potentiometer after the cleaning of the surface. The linear potentiometer is fixed in such a way that it is independent of the girder vibrations and other movements. The platform to support the linear potentiometer is made to be even, and the same is checked with the spirit level. The linear potentiometer is clamped on its stand which is fixed and secured with the platform. The contact with the bottom chord of the girder is established with the head of the plunger such that the initial reading is recorded with the corresponding change in the voltage. The TIPO PM 25 5K MR Potentiometer was used.

This is concluding sentence about the deflection values recorded in left span of girder no 2 under dynamic and static loading condition and successfully conveyed its message (Figs. 14 and 15).

The measurement of the natural frequency of the RCC girders simply supported over piers was done at mid-span for one cracked span and one un-cracked PSC I girders in the two spans. Prestressed concrete (PSC) bridge girders no. 114 UP has undergone distress with age through the loss of prestressing force and through the development of structural cracks in the concrete. It is expected that such a distress will be reflected through a change of stiffness of the girder [19]. The motion (or dynamic force) of the vibrating body is converted into an electrical signal by the vibration transducer or pickup. The accelerometer is attached to the metal base plate using the magnetic property. The accelerometer B&K model no. 4396 is used for recording the vibration. The vibrations in the girder are measured by the accelerometer in an acceleration versus time-domain graph using National Instruments DGC cDAQ 9178 & National Instruments module 9025 along with accelerometer B&K model no. 4396. The locomotive WAG 7 was moved over the girder. The corresponding vibrations in the girder were recorded in the software. These data are converted into an acceleration vs frequency domain graph using the fast Fourier transform (FFT) algorithm. DGC cDAQ Software is incorporated for processing of signals and the FFT of the acquired data. The software algorithm is available in the form of block which has the formulation for carrying out the FFT of the acquired. The data are analyzed in various segments and

Table 8 Post-strengthening test results

S. No.	Span no.	Girder no.	Type of loading	Deflection (mm)	Natural frequency (Hz)	Test result after strengthening (days)
1	2	RSG	Dynamic@20 kmph	2.789	9.481	28
2	2	LSG	Dynamic@20 kmph	3.2425	9.0961	28
3	2	Avg.	Dynamic@20 kmph	3.01575	9.28855	28
4	2	RSG	Static	2.8768	NA	28
5	2	LSG	Static	3.285	NA	28
6	2	Avg.	Static	3.0809	NA	28
7	4	RSG	Dynamic@20 kmph	3.809	8.248	10
8	4	LSG	Dynamic@20 kmph	4.413	9.149	10
9	4	Avg.	Dynamic@20 kmph	4.111	8.6985	10
10	4	RSG	Static	3.864	NA	10
11	4	LSG	Static	4.442	NA	10
12	4	Avg.	Static	4.153	NA	10
13	2	RSG	Dynamic@20 kmph	2.8943	8.4329	139
14	2	RSG	Dynamic@100 kmph	2.8021	8.7184	139
15	2	LSG	Dynamic@20 kmph	3.2804	8.7298	139
16	2	LSG	Dynamic@100 kmph	3.3976	8.5416	139
17	2	RSG	Static	2.9161	NA	139
18	2	LSG	Static	3.3575	NA	139
19	2	Avg.	Dynamic@20 kmph	3.08735	8.58135	139
20	2	Avg.	Dynamic@100 kmph	3.09985	8.63	139
21	2	Avg.	Static	3.1368	NA	139
22	4	RSG	Dynamic@20 kmph	3.113	9.0021	139
23	4	RSG	Dynamic@100 kmph	3.229	9.2031	139
24	4	LSG	Dynamic@20 kmph	3.1794	8.9129	139
25	4	LSG	Dynamic@100 kmph	3.2966	8.3321	139
26	4	RSG	Static	3.1947	NA	139
27	4	LSG	Static	3.3339	NA	139
28	4	Avg.	Dynamic@20 kmph	3.1462	8.9575	139
29	4	Avg.	Dynamic@100 kmph	3.2628	8.7676	139
30	4	Avg.	Static	3.2643	NA	139
31	2	LSG	Static	3.62	NA	309
32	2	LSG	Dynamic@100 kmph	3.58	9.0285	309
33	2	RSG	Static	3.55	NA	309
34	2	RSG	Dynamic@100 kmph	3.5	9.3308	309
35	2	Avg.	Static	3.585	NA	309
36	2	Avg.	Dynamic@100 kmph	3.54	9.17965	309
37	4	RSG	Static	3.34	NA	309
38	4	RSG	Dynamic@20 kmph	3.3	8.8796	309
39	4	LSG	Static	2.92	NA	309
40	4	LSG	Dynamic@20 kmph	3	8.4847	309
41	4	Avg.	Static	3.13	NA	309
42	4	Avg.	Dynamic@20 kmph	3.15	8.68215	309
43	2	LSG	Static	3.3018	NA	481
44	2	LSG	Dynamic@20 kmph	3.3053	8.6694	481
45	2	LSG	Dynamic@100 kmph	3.3566	8.7056	481
46	2	RSG	Static	2.8216	NA	481
47	2	RSG	Dynamic@20 kmph	2.7444	8.4524	481
48	2	RSG	Dynamic@100 kmph	2.6732	8.6926	481

Table 8 continued

S. No.	Span no.	Girder no.	Type of loading	Deflection (mm)	Natural frequency (Hz)	Test result after strengthening (days)
49	2	Avg.	Static	3.0617	NA	481
50	2	Avg.	Dynamic@20 kmph	3.02485	8.5609	481
51	2	Avg.	Dynamic@100 kmph	3.0149	8.6991	481
52	4	LSG	Static	3.2751	NA	481
53	4	LSG	Dynamic@20 kmph	3.308	8.68	481
54	4	LSG	Dynamic@100 kmph	3.2609	8.6926	481
55	4	RSG	Static	3.3	NA	481
56	4	RSG	Dynamic@20 kmph	3.1717	8.9764	481
57	4	RSG	Dynamic@100 kmph	3.1413	9.07	481
58	4	Avg.	Static	3.28755	NA	481
59	4	Avg.	Dynamic@20 kmph	3.23985	8.8282	481
60	4	Avg.	Dynamic@100 kmph	3.2011	8.8813	481

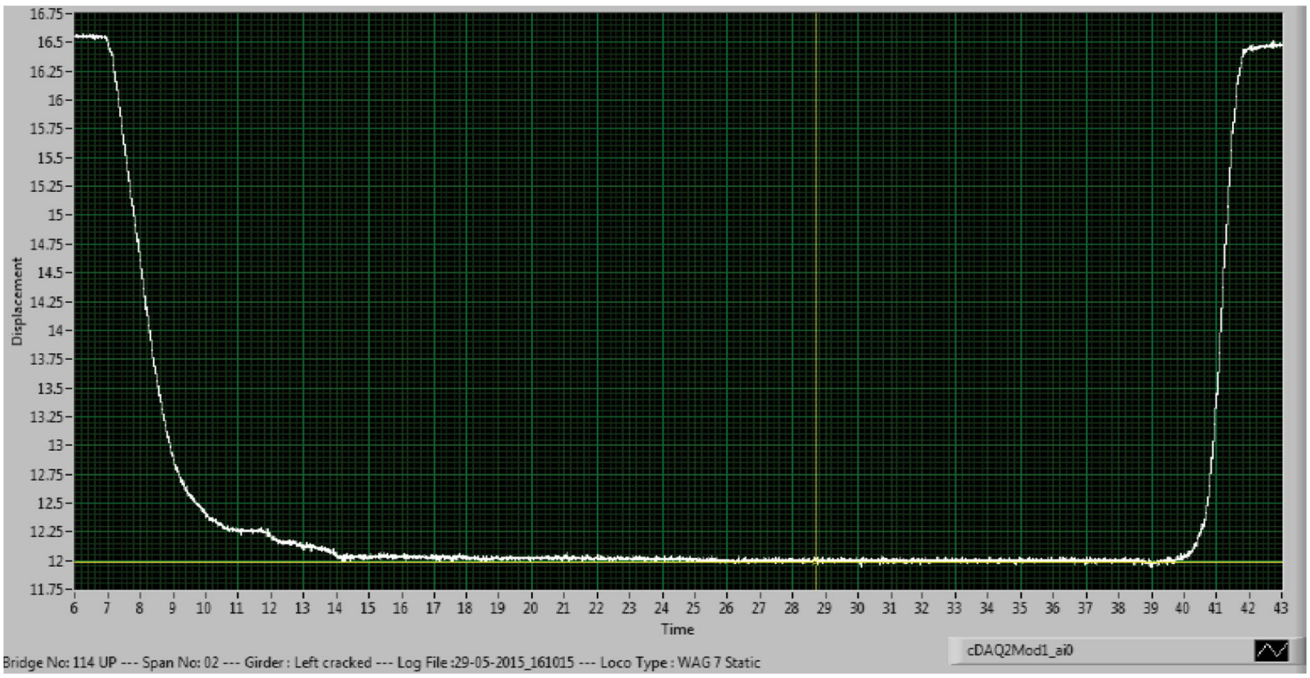

Fig. 15 Maximum deflection of cracked left girder static load on span no. 2

are cropped to get the modal participation of the desired frequency.

Similarly, also the pre-strengthening test results recorded on the various spans of bridge 114 for natural frequencies are listed in Table 7. The maximum natural frequency (9.57 Hz) in un-cracked condition was recorded on the right-side girder of span no. 1 under dynamic loading condition (Fig. 16).

(ii) Post-strengthening test results

The post-strengthening data for deflection and natural frequencies were recorded for 481 days. Few of the critical results are presented in this section to show the behavior of bridge. The mid-span deflection of the girder was recorded and is presented in Figs. 20 and 21 for dynamic and static loading, respectively. The maximum deflection observed 4.413 mm for dynamic loading condition and 4.442 mm for static loading which are shown in Figs. 17 and 18, respectively.

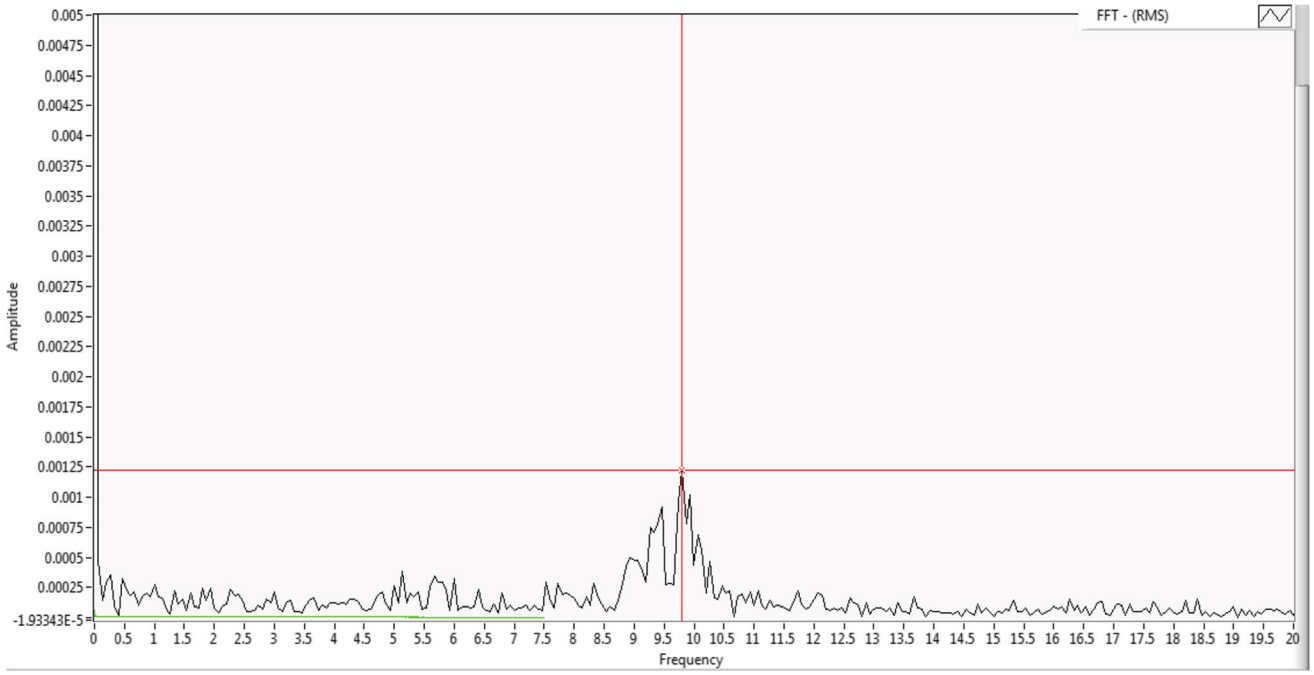

Fig. 16 Amplitude vs. frequency of right girder on dynamic load

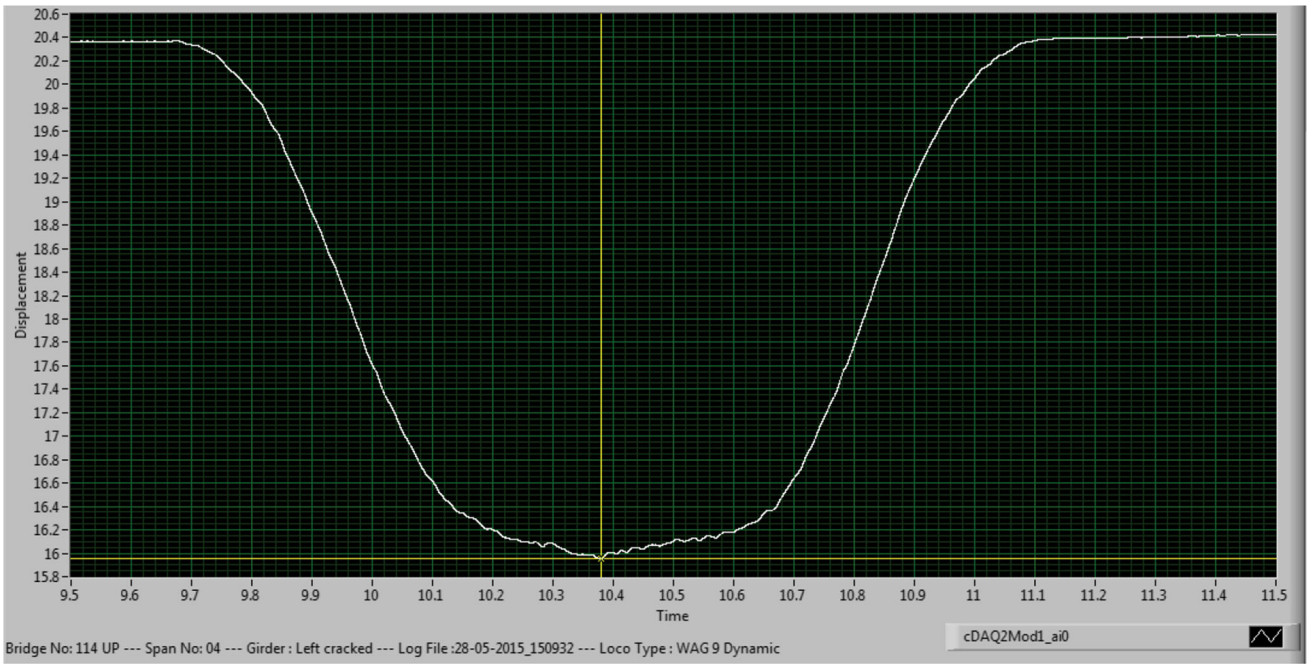

Fig. 17 Deflection curve of post-strengthening girder no. 4 with dynamic loading

Post-strengthening Test Results for Natural Frequency

All the tests performed on the bridge to obtain natural frequency of girder after repairing of damaged bridge are listed in Table 8. Figure 19 represents the change of frequency with amplitude that corresponds to the maximum recorded frequency of 9.481 Hz.

This study comprises the behavior and performance of bridge girder before and after strengthening. Girder no. 1 was undamaged and was not repaired, so it was tested only once. Figure 20 shows the mean deflection recorded before and after strengthening of the second and fourth span of bridge. It can be concluded that the percentage decrement in deflection is 20.08% and 21.98 in the second and fourth

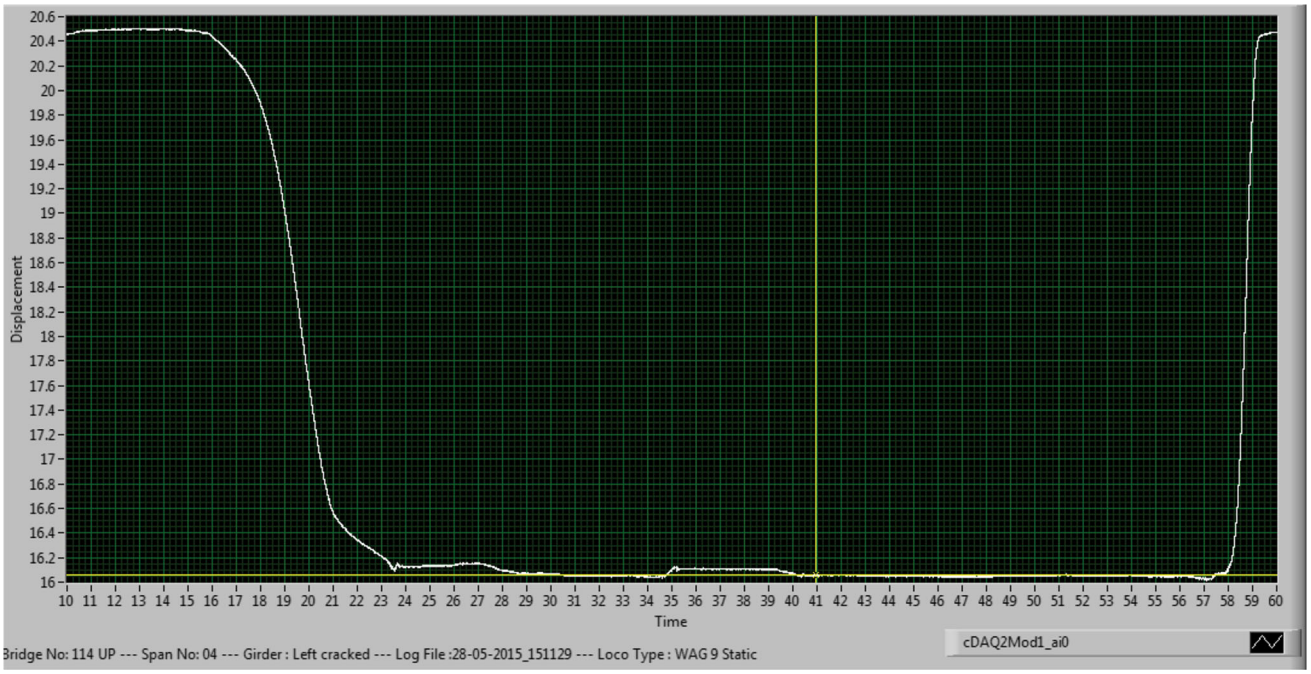

Fig. 18 Deflection curve of post-strengthening girder no. 4 with static loading

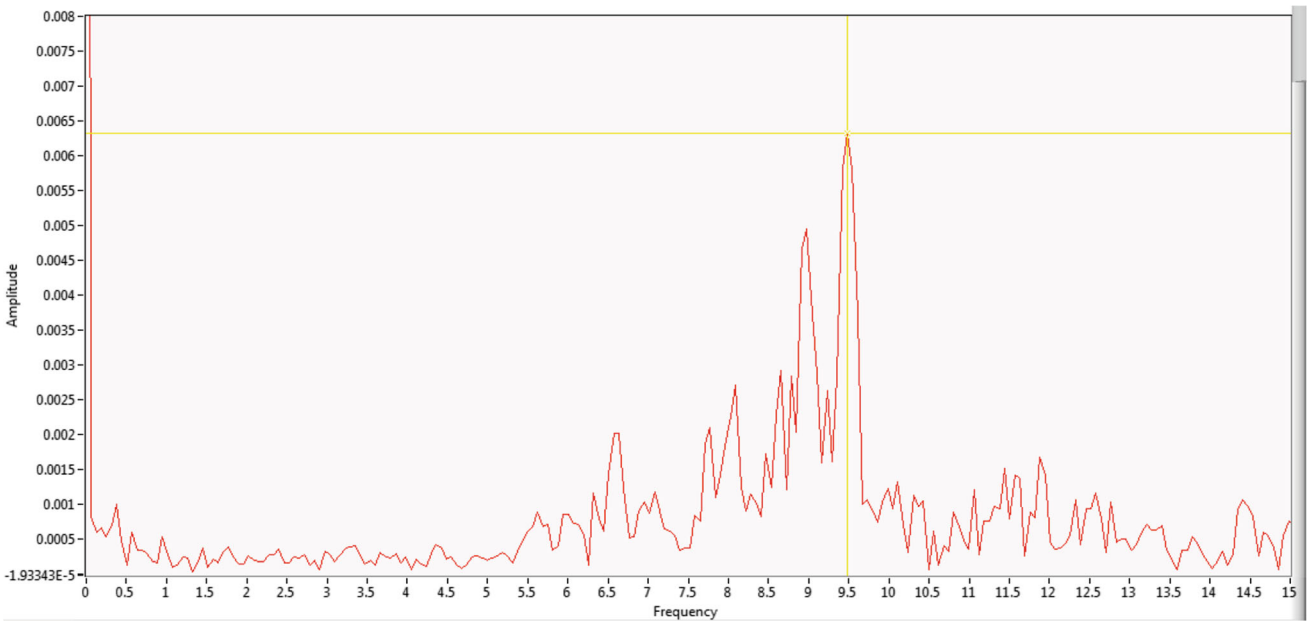

Fig. 19 Amplitude vs. frequency of right girder of span 2 under dynamic loading

girders, respectively. Figure 21 shows the deflection of girder in the dynamic loading of Indian rail locomotive, while Fig. 22 contains the natural frequency data of pre- and post-repairing. It shows that the percentage increment in natural frequency after strengthening is 3.20% and 7.52 in the second and fourth girders, respectively, after 481 days.

Conclusions

The post-strengthening test result of static and dynamic behavior of bridge no. 114 over Khan river has been studied extensively which reveals the suitability and better serviceability of carbon and glass fiber to the reinforced concrete for the better performance. Based on the above test, the following conclusion can be drawn:

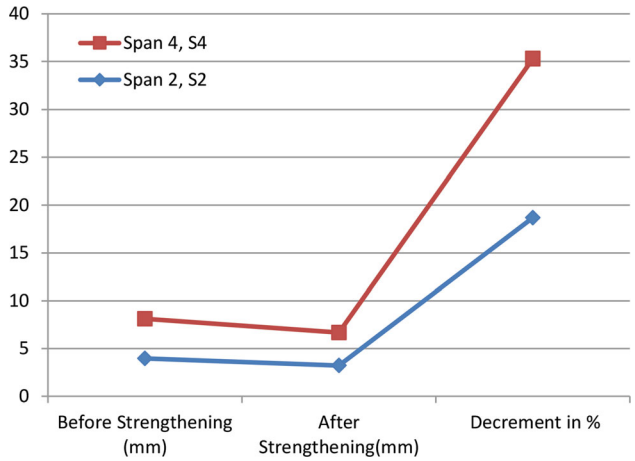

Fig. 20 Analysis of static deflection of girder

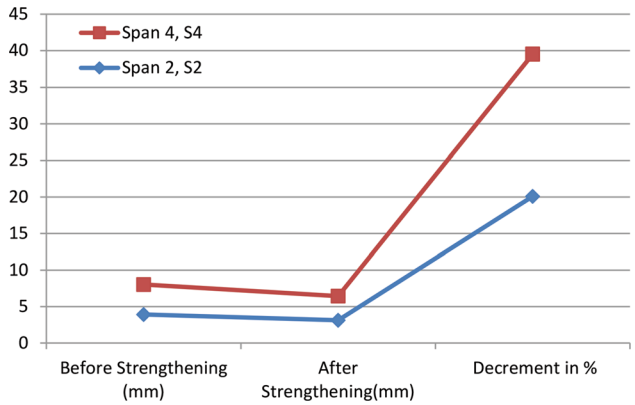

Fig. 21 Analysis of dynamic deflection of girder

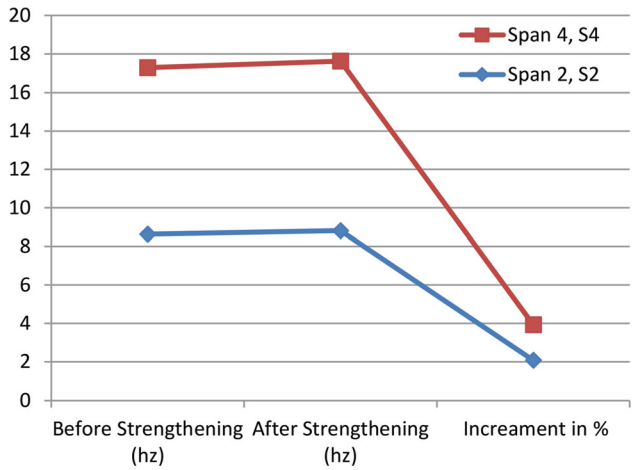

Fig. 22 Analysis of natural frequency of girder

1. After strengthening, reductions in static deflection were recorded in span 2 of the girder by an average of 18.69% as compared to that recorded in initial cracked position before strengthening. And after strengthening, there is an average of 16.63% reduction in static deflection in the girder of span no. 4 as compared to that recorded in initial cracked position before strengthening.
2. After strengthening, reductions in dynamic deflection were recorded in span 2 of the girder by an average of 20.08% as compared to that recorded in initial cracked position before strengthening. And after strengthening, there is an average of 19.46% percentage reductions in dynamic deflection in the girder of span no. 4 as compared to that recorded in initial cracked position before strengthening.
3. Natural frequency of un-cracked girder is more than the natural frequency of cracked girder, indicating that an un-cracked girder has enhanced stiffness compared to the cracked girder. After strengthening, the average percentage of the natural frequency of the cracked span no. 2 girders is increased by 2.08% in comparison with that recorded in cracked condition before strengthening. And after strengthening the girder, the average percentage of the natural frequency of the cracked span no. 4 increased to 1.85% in comparison with cracked condition before strengthening. The natural frequency of cracked girder has been improved and brought very close to that of the un-cracked girder.
4. Before strengthening, the speed restriction was 20 km/h, and now after strengthening the allowable maximum speed of the train is 100 km/h. Due to increment above two, the speed restriction removed, resulted in saving of 17 min during the passing of this bridge.

References

1. H. Saadatmanesh, M.R. Ehsani, RC beams strengthened with GFRP plates. I: experimental study. J. Struct. Eng. **117**, 3417–3433 (1991)
2. Ross et al., Hardening and rehabilitation using frp.pdf (n.d.)
3. S. Jm, T. Jw, E field performance of FRP bridge repairs. J. Bridge Eng. **5**, 107–133 (2000)
4. J.R. Yost, E.R. Schmeckpeper, Strength and serviceability of FRP grid reinforced bridge decks. J. Bridge Eng. **6**, 605–612 (2001)
5. T.C. Miller, M.J. Chajes, D.R. Mertz, J.N. Hastings, Strengthening of a steel bridge girder using CFRP plates. J. Bridge Eng. **6**, 514–522 (2001)
6. U. Meier, H. Kaiser, Strengthening structures with CFRP laminates. Adv. Compos. Mater. Bridge Struct. **1**, 224–232 (1991)
7. M.S. Saiidi, R. Johnson, E.M. Maragakis, Development, shake table testing, and design of FRP seismic restrainers. J. Bridge Eng. **11**, 499–506 (2006)
8. American Association of State Highway and Transportation Officials (AASHTO), *AASHTO LRFD bridge design specification—SI unit, 1998 (2003 interim revisions)*, 2nd Ed. (Washington, DC, 2003)
9. Y. Zhang, C.S. Cai, X. Shi, Vehicle load-induced dynamic performance of FRP slab. Bridges **11**, 1–10 (2006)
10. T.H. Miller, K. Chansawat, T. Potisuk, S.C. Yim, D.I. Kachlakev, FE models of GFRP and CFRP strengthening of reinforced

concrete beams. Adv. Civ. Eng. (2009). https://doi.org/10.1155/2009/152196
11. K. Siamardi, A.A. Mounesan, M.M.K. Zanjan, Application of fiber reinforced plastics for concrete T-beam bridge strengthening, in *3rd International Conference on Concrete and Development, Iran symposia, 1–6, 2009*. http://www.civilica.com/Paper-ICCD03-ICCD03_071.html
12. M. Noël, K. Soudki, Evaluation of FRP posttensioned slab bridge strips using AASHTO-LRFD bridge design specifications. J. Bridge Eng. **16**, 839–846 (2011)
13. S.-W. Bae, A. Belarbi, Behavior of various anchorage systems used for shear strengthening of concrete structures with externally bonded FRP sheets. J. Bridge Eng. **18**, 837–847 (2012)
14. W.-W. Wang, J.-G. Dai, K.A. Harries, Performance evaluation of RC beams strengthened with an externally bonded frp system under simulated vehicle loads. J. Bridge Eng. **18**, 76–82 (2011)
15. J. Michels, M. Staśkiewicz, C. Czaderski, R. Kotynia, Y.E. Harmanci, M. Motavalli, Prestressed CFRP strips for concrete bridge girder retrofitting: application and static loading test. J. Bridge Eng. **21**, 04016003 (2016)
16. R.D.A.S. Organisation, Technical Specification for Development of Re-generative Braking Feature in WAG7 Electric Locomotives, Government of India Ministry of Railways. RDSO/2018/(2018), pp. 1–42
17. IRC:112-2011, *Code of Practice for Concrete Road Bridges* (Indian Road Congress, New Delhi, 2011)
18. H.S. Birajdar, P.R. Maiti, P.K. Singh, Failure of Chauras bridge. Eng. Fail. Anal. **45**, 339–346 (2014)
19. A.K. Shukla, P.R. Maiti, Retrofitting and rehabilitation of damage footbridge over Yamuna River. Int. J. Recent Technol. Eng. **8**(2), 4239–4246 (2019)